J Mater Sci: Mater Med (2010) 21:815–821
DOI 10.1007/s10856-009-3882-2

Frictional properties of light-activated antimicrobial polymers in blood vessels

Polina Prokopovich · Stefano Perni · Clara Piccirillo · Jonathan Pratten · Ivan P. Parkin · Michael Wilson

Received: 3 July 2009 / Accepted: 17 September 2009 / Published online: 27 September 2009

Abstract The adhesion of microbes to catheter surfaces is a serious problem and the resulting infections frequently lead to longer hospitalisation and higher risk for the patient. Several approaches have been developed to produce materials that are less susceptible to microbial colonisation. One such approach is the incorporation of photoactivated compounds, such as Toluidine Blue O (TBO), in the polymeric matrix resulting in 'light-activated antimicrobial materials'. The insertion and removal of catheters can cause tissue damage and patient discomfort through frictional forces; hence the lubricity of a catheter material is also very important. In this work the tribological performance of silicone and polyurethane containing TBO and gold nanoparticles were evaluated using two different surfaces, the inner part of the aorta and the superior vena cava of sheep. Static and kinetic friction coefficients of these materials were measured using a tribometric device developed for in vitro applications using dry materials and those lubricated with blood. It was found that neither the preparation process nor the presence of TBO or gold nanoparticles, had an effect on the friction factors in comparison to those of untreated materials. In all cases, static and kinetic friction coefficients on aorta tissue were higher than those on vena cava due to higher surface roughness of the aorta. The presence of blood as a lubricant resulted in lower friction coefficients.

P. Prokopovich
Wolfson School of Mechanical and Manufacturing Engineering, Loughborough University, Loughborough LE11 3TU, UK

S. Perni · J. Pratten · M. Wilson (✉)
Division of Microbial Diseases, UCL Eastman Dental Institute, University College London, 256 Grays Inn Road, London WC1X 8LD, UK
e-mail: m.wilson@eastman.ucl.ac.uk

C. Piccirillo · I. P. Parkin
Department of Chemistry, Materials Chemistry Research Centre, University College London, 20 Gordon Street, London WC1H OAJ, UK

1 Introduction

Solid–solid friction is a complex and universal phenomenon that is found at various scales from the atomic to the macroscale [1, 2]. Friction is the result of the simultaneous action of various mechanisms such as adhesion and deformation of asperities (ploughing) [3, 4]. These various mechanisms lead to a dissipative process which is characterised by a single parameter, the coefficient of friction, which is equal to the ratio between the friction force and the normal load [5, 6]. The coefficient of friction "*f*" is categorized as either static or kinetic. The coefficient of static friction occurs when no movement exists between the two surfaces, and the kinetic coefficient of friction takes place when motion occurs. The coefficient of static friction is usually greater than the coefficient of kinetic friction [7]. The coefficient of friction in the dry case is independent of the normal load, nominal size of contact and sliding velocity, whilst the coefficient of friction in lubricated conditions may strongly depend on normal load and sliding velocity, this dependence is usually described using the Stribeck diagram.

Catheters are routinely employed medical devices through which flow biological fluids such as blood or urine. When these fluids contain microorganisms the latter can adhere to the surface producing a biofilm which have a very low susceptibility to antimicrobial agents [8–10]. The resulting infections frequently lead to longer hospitalisation and higher risk for the patient [11].

A lot of research has been devoted to the preparation of materials that can inhibit or reduce microbial surface colonisation. This can be achieved by coating with Ag nanoparticles or by incorporation of antibiotics [12, 13]. More recently, photoactivated materials have been proposed [14, 15]. These exert an antimicrobial effect by generating reactive oxygen species in the presence of light. The light-activated antimicrobial (LAA) toluidine blue O (TBO) and Methylene blue have been successfully incorporated into silicone and polyurethane [14, 15] resulting in materials with antimicrobial properties when irradiated with light, moreover these antimicrobial properties can be enhanced by the presence of gold nanoparticles [14].

Another important aspect to be investigated is the effect that incorporation of LAA into catheter material has on the catheter friction factors. These are important measurements as catheter insertion and removal induces frictional forces that cause damage to the surrounding tissues and lead to patient discomfort. Indeed, an assessment of the lubricity of the catheter surface is often carried out to screen different catheters materials [16–18]. Moreover, knowledge of the lubricity is essential to determine the clinical potential of a new catheter material.

In this work, silicone and polyurethane containing TBO and gold nanoparticles were tested against the inner part of aorta and vena cava obtained from lambs. Static and kinetic friction coefficients of these materials were measured using a tribometric device developed for in vitro applications using both dry and lubricated materials.

2 Materials and methods

2.1 Polymer preparation

Silicone elastomers were prepared using liquid MED-4850 (Polymer Systems Technology Ltd.) as a starting material; this was mixed with the crosslinking agent in a 1:1 ratio, and spread uniformly on to a glass surface to make a 1 mm thick sheet. The polymer was cured at 80°C for 2.5 h, allowed to cool and then the sheet was cut into smaller coupons (squares 1.0×1.0 cm^2). Polyurethane samples were also cut into 1.0×1.0 cm^2 coupons from a sheet (thickness 0.8 mm) purchased from American Polyfilm Inc. (Branford, CT, USA). Both these polymers were medical grade silicone and polyurethane respectively.

TBO (Sigma, UK) solutions were prepared at a concentration of 500 ppm in acetone:distilled-H_2O or in acetone: aqueous Au-nanoparticles, in both cases the ratio was 9:1 acetone:aqueous solution. The solutions were sonicated in an ultrasound bath for 15 min to ensure complete TBO dissolution. Au nanoparticles were purchased from BBInternational Ltd. (Cardiff, UK) and were stated to be 2 nm in diameter and a concentration of 1.5×10^{14} particles/ml.

Polymer samples were prepared, embedded either with TBO only (TBO + Au−), TBO and Au nanoparticles (TBO + Au +) or nanoparticles only (TBO − Au +). In all cases, a 1.0 cm square sample was placed into the appropriate solution and left to swell in the dark for 24 h inside a closed bottle containing 10.0 ml of the TBO solution. After this the samples were left to dry in the dark at room temperature for 24 h. Two blanks were prepared, a polymer sample not swollen in any solvent and one swollen in solvent and allowed to evaporate.

2.2 Principle of the tribometric device operation

A scheme of the tribometric device is shown in Fig. 1. It measures the force required to drag, at a known velocity, a load cell containing the surface to be tested, across the static counter surface.

Raw friction data (in volts) and sliding velocity (in volts) were observed on the graph and recorded in real time. The sliding velocity was recorded by a laser vibrometer (model Polytec 302, Polytec, UK). Knowing the sensitivity (25.0 mm/s/V) of the vibrometer controller, the sliding velocity was converted into mm/s. A calibration procedure was adopted to convert friction signals from volts into Newtons. Before the experiments, a load cell (model 1004, capacities: 0.3–3 kg, Tedea-Huntleigh Europe Ltd., Cardiff, UK) was calibrated with known weights to obtain the friction sensitivity. All raw friction force values (in volts) were multiplied by the friction sensitivity (1.18 N/V) to convert them to the friction force in units of N. Friction coefficients were obtained by dividing the friction force by the applied normal load according to Amonton's Law [5]. The sliding velocity of one counter surface against another was constant and equal to 0.03 m/s, whilst the applied normal load was 4 N.

The outputs from the force transducers, which are fed to the vibrometer controller, were analysed using a software program written in LabView 7.1.

2.3 Surface roughness analysis

Surface roughness measurements of the polymeric materials and blood vessels were obtained using Talysurf CLI 2000 scan at 100 μm scan speed at spacing along the x-axis equal 0.5 μm and along y-direction equal 2 μm. A total area of 1.0×1.0 cm^2 was scanned for each sample before and after the friction test was performed. The average surface value (Ra) was calculated as the average of five scans on three independent samples.

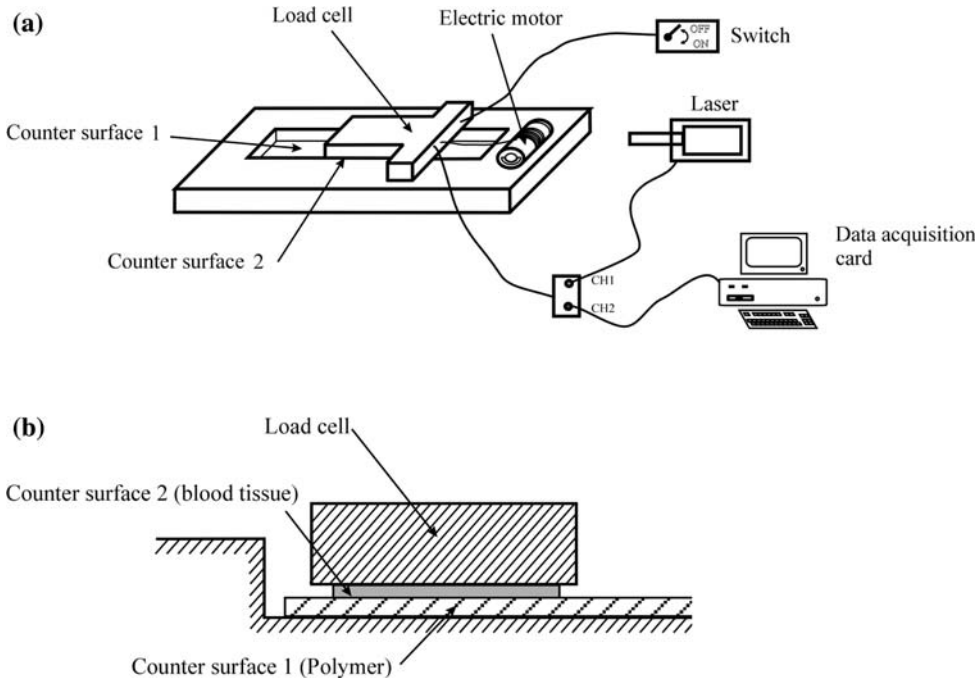

Fig. 1 Schematic representation (**a**) and section (**b**) of the tribometric device

2.4 Aorta and vena cave tissue preparation

Heart with connected aorta and vena cava from lambs were purchased from a local butcher on the day of slaughter and kept at Phosphate Buffer Solution (PBS, Oxoid) at 4°C for no more than 1 h during transportation. As soon the samples reached the lab, aorta and vena cava were detached from the heart with a scalpel and washed three times in fresh sterile PBS; pieces of aorta and vena cava with a length of approximately 4 cm were cut along the main axis to obtain a rectangular-shaped piece that was left in PBS at 37°C for 20 min and then attached to the tribometric device.

Defibrinated horse blood (DHB100, E&O Laboratories Limited, Burnhouse, Scotland) was used as a lubricant. The blood was stored at 4°C for no more than 1 week and equilibrated at 37°C for 2 h before use in the experiments.

All measurements were performed at ambient temperature and 45% RH. It has been reported previously that the friction characteristics of the tissue are not affected by temperature in the range 19–39°C [19]. Measurements were performed using aorta and vena cava from three different specimens and three independent material samples.

2.5 Statistical methods

The values of the friction factors from each of the two untreated materials were compared with the values of the same treated material using the one-way ANOVA test followed post-hoc by the Tukey's test for individual pairs of data sets. These analyses were performed using SPSS 14.0 software (SPSS Inc., Chicago, IL, USA).

3 Results and discussion

In this work the effect of encapsulating LAA in polyurethane and silicone on the friction factor of the materials has been determined on squares samples as catheters of these materials are not available yet, furthermore the benefit of an in vivo approach rather than other tests in assessing the friction properties of newly developed catheters is unclear [16].

The friction coefficient in lubricated conditions depends on the ratio of the lubricant film thickness and composite surface roughness, this parameter is called (λ). In case of catheters, these conditions correspond to the boundary lubrication region of the Stribeck curve [20, 21] described by $\lambda < 1$. Therefore, in this work, tests have been conducted only under experimental conditions representing boundary lubrication. The λ value was determined estimating the film thickness according to the Karaszkiewicz's equation [22] and using the experimentally measured values of surface roughness to determine the composite surface roughness between the two counter-surfaces as follow:

$$R_{a,comp} = \sqrt{R_{a1}^2 + R_{a2}^2} \quad (1)$$

In all cases the value of λ calculated was below 1.

Previous work on silicone with embedded Methylene Blue showed that the main effect of the preparation method on the surface roughness and Young's modulus was attributable to the swelling/shrinking process alone, whilst the presence of the photosensitiser did not affect the mechanical properties any further [14]. The model surfaces

chosen for this study, aorta and vena cava, were selected as representative of the two major types of blood vessel, arteries and veins. Models that do not employ animal tissues are available for the bladder (based on Agar solution [16] or porcine gastric mucine [17]), but not for blood vessels. Furthermore, porcine aorta has previously been used to determine the friction factors associated with intravenous catheters [21].

The profile of the friction factor of polyurethane using aorta tissue is shown in Fig. 2. Initially there was a constant increase up to a maximum that represents the static friction factor. Only when the curve reaches the maximum, the value of the applied force equals the frictional force and can be used to calculate the static friction coefficient by dividing the measured force by the normal load, for this reason the initial tract of the plot in Fig. 2 is presented with a dashed line for the dry case and dashed-dotted for the lubricated case. After this, the load cell starts moving and the friction factor decreases and starts oscillating around the kinetic friction factor. The oscillations during the movement of the load cell are due to stick/slip phenomena. This behaviour is typical and was also found in other investigations of the friction properties of catheters [18, 21, 23].

Friction factor values of the polymer materials against aorta tissue are presented in Table 1. ANOVA analysis revealed that untreated silicone and polyurethane did not have different friction factors from those of the treated materials, this occurred for both the dry and lubricated materials as well as for the static and kinetic coefficients ($P < 0.05$). For each of the five silicone and five polyurethane materials tested, the static coefficient was higher than the corresponding kinetic one, both in the dry and lubricated case.

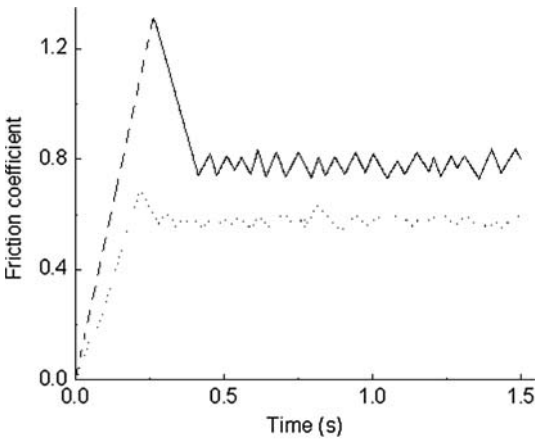

Fig. 2 Example of dependence of friction coefficients in aorta with time of polyurethane for dry (*continuous line*) and lubricated material (*dotted line*)

Kazmierska et al. [21] measured the friction coefficient of a commercial silicone catheter against porcine aorta, lubricated with distilled water, and reported a static friction factor of 0.1 and a kinetic friction factor of 0.05. These lower values can be attributed to the different lubricant used, in the present study blood was employed as it is the fluid encountered in blood vessels and it is more appropriate than water for estimating the friction factor of intravenous catheters. Moreover, the focus of this study was to determine the effect of the embodiment of LAA on the friction properties of medical grade silicone and polyurethane not just to estimate their friction factors values.

Table 2 shows the friction factors values of the photosensitiser-containing materials against vena cava tissue. Again, similar to the aorta work, the ANOVA analysis revealed that untreated silicone and polyurethane have similar friction factors to those of the treated materials, this happened both in the dry and lubricated case and for the static and kinetic friction coefficients ($P < 0.05$). For each of the five silicone and five polyurethane materials tested, the static friction coefficient was higher than the corresponding kinetic one in both the dry and lubricated cases.

It is well known that the values of the coefficient of friction, when measured at the micro/nanoscale, can be different from those determined at a macroscale, and therefore friction is scale-dependent [24–27]. However, the findings presented in this work, obtained at a macro scale level, are in agreement with those of Perni et al. [15] which employed AFM (nanoscale level) to determine the friction coefficient of the polymers with embedded LAA and reported that the encapsulation of LAA did not have a significant effect on the friction properties. However, the friction coefficients values are different as a consequence of the different counter surface used in the two studies.

The surface roughness of the polymers with embedded LAA is shown in Table 3. From this table, it can be seen that the swelling mechanism alone is responsible for an increase in the surface roughness ($P < 0.05$). It also shows that the surface roughness of the materials is reduced after the test ($P < 0.05$); moreover the reduction is higher after a dry friction test than after a lubricated friction test ($P < 0.05$).

The friction forces generated during the contact between a surface and biological tissues are capable of causing surface deformation [4]; this deformation is responsible for the reduction in surface roughness reported in Table 3. Moreover, similar to the lubricated case, the friction forces are lower, further demonstrated by a lower friction coefficient; the deformation caused a smaller Ra reduction.

Friction tests of both silicone and polyurethane-based materials against the vena cava revealed a reduction of both static and kinetic friction coefficients in comparison with the friction results obtained on the aorta tissue. In the non-lubricated case, a reduction of the static friction

Table 1 Friction coefficients of silicone and polyurethane samples using aorta

Material	Dry		Lubricated	
	Static friction coefficient	Kinetic friction coefficient	Static friction coefficient	Kinetic friction coefficient
Silicone				
Untreated	1.30 ± 0.02	0.78 ± 0.02	0.67 ± 0.02	0.57 ± 0.02
Swollen acetone:water	1.35 ± 0.03	0.80 ± 0.02	0.71 ± 0.02	0.55 ± 0.02
Swollen acetone:Au	1.32 ± 0.02	0.76 ± 0.02	0.56 ± 0.03	0.51 ± 0.02
TBO	1.21 ± 0.01	0.61 ± 0.02	0.58 ± 0.02	0.45 ± 0.02
TBO + Au	1.27 ± 0.02	0.65 ± 0.02	0.51 ± 0.01	0.46 ± 0.03
Polyurethane				
Untreated	1.35 ± 0.01	1.00 ± 0.03	0.78 ± 0.04	0.31 ± 0.03
Swollen acetone:water	1.34 ± 0.02	0.98 ± 0.02	0.74 ± 0.02	0.27 ± 0.03
Swollen acetone:Au	1.29 ± 0.03	0.87 ± 0.01	0.76 ± 0.02	0.25 ± 0.01
TBO	1.26 ± 0.02	0.83 ± 0.02	0.58 ± 0.02	0.23 ± 0.02
TBO + Au	1.26 ± 0.01	0.87 ± 0.01	0.65 ± 0.02	0.25 ± 0.01

Table 2 Friction coefficients of silicone and polyurethane samples using vena cava

Material	Dry		Lubricated	
	Static friction coefficient	Kinetic friction coefficient	Static friction coefficient	Kinetic friction coefficient
Silicone				
Untreated	1.01 ± 0.03	0.75 ± 0.02	0.56 ± 0.01	0.20 ± 0.02
Swollen acetone:water	0.97 ± 0.01	0.77 ± 0.02	0.51 ± 0.02	0.21 ± 0.01
Swollen acetone:Au	0.97 ± 0.01	0.66 ± 0.02	0.46 ± 0.01	0.17 ± 0.01
TBO	0.95 ± 0.01	0.63 ± 0.01	0.41 ± 0.02	0.16 ± 0.01
TBO + Au	0.96 ± 0.01	0.61 ± 0.02	0.43 ± 0.01	0.18 ± 0.01
Polyurethane				
Untreated	0.91 ± 0.02	0.71 ± 0.02	0.56 ± 0.01	0.42 ± 0.02
Swollen acetone:water	0.92 ± 0.01	0.72 ± 0.03	0.62 ± 0.02	0.44 ± 0.02
Swollen acetone:Au	0.87 ± 0.01	0.68 ± 0.01	0.62 ± 0.02	0.46 ± 0.01
TBO	0.85 ± 0.02	0.61 ± 0.02	0.48 ± 0.01	0.36 ± 0.01
TBO + Au	0.88 ± 0.01	0.65 ± 0.01	0.54 ± 0.01	0.41 ± 0.02

coefficient was 25–30% and the kinetic friction coefficient decreased by up to 25%.

This is probably due to the different surface structures of the aorta and vena cava [28]. This structural difference is also reflected in different values of *Ra* for the two tissues, 1.044 ± 0.016 and 0.434 ± 0.008 μm respectively.

The increased friction against an aorta is due to the fact than the higher the surface roughness then the higher is the area of contact between the two surfaces [1]. Therefore, the forces which originate at the interface between the LAA-containing materials and the aorta are higher than those between the LAA-containing materials and the vena cava.

This correlation was not found for the friction coefficients of silicone and polyurethane containing TBO and gold nanoparticles; the increase of surface roughness in the polymers with TBO compared to the untreated ones (Table 3) did not result in any increase in the friction coefficients of silicone or polyurethane using aorta or vena cava tissue. This is probably due to the relatively small increase in the surface roughness in the treated samples compared to the ratio of the surface roughnesses of the aorta and vena cava.

Surface hydrophilicity of intravenous and urological catheters has been related to lower friction [29, 30], however Perni et al. [15] has shown that the presence of TBO in silicone and polyurethane promote a more hydrophobic surface. This seems to agree with the findings of Jones et al. [16] that neglected the effect of contact angle of water

Table 3 Surface roughness before and after friction test of silicone and polyurethane samples and aorta or vena cava as counter surfaces

Material	*Ra* (μm) before friction test	*Ra* (μm) after dry friction test	*Ra* (μm) after lubricated friction test
Silicone			
Untreated	0.031 ± 0.004	0.023 ± 0.004	0.027 ± 0.002
Swollen acetone:water	0.052 ± 0.002	0.038 ± 0.002	0.045 ± 0.002
Swollen acetone:Au	0.045 ± 0.002	0.032 ± 0.003	0.038 ± 0.002
TBO	0.041 ± 0.003	0.029 ± 0.003	0.035 ± 0.002
TBO + Au	0.042 ± 0.003	0.031 ± 0.002	0.036 ± 0.002
Polyurethane			
Untreated	0.191 ± 0.011	0.137 ± 0.021	0.168 ± 0.020
Swollen acetone:water	0.292 ± 0.010	0.215 ± 0.023	0.249 ± 0.056
Swollen acetone:Au	0.231 ± 0.011	0.164 ± 0.028	0.201 ± 0.018
TBO	0.281 ± 0.009	0.131 ± 0.024	0.159 ± 0.022
TBO + Au	0.252 ± 0.011	0.184 ± 0.016	0.224 ± 0.020

on the catheters lubricity but reported the surface roughness as the main controlling parameter. As previously stated, the variation in surface roughness as a consequence of the preparation method is relatively small and therefore the effect on the friction coefficients has not been detectable.

4 Conclusion

The friction coefficients of silicone and polyurethane after incorporation of TBO via a swelling/shrinking process are the same as those of the untreated polymers. This is extremely important as patient comfort during insertion and removal is one of the key factors in developing new materials for use as catheters, as high friction coefficients are a source of discomfort and pain. Our results suggest that TBO-containing silicone and polyurethane do not generate more friction than the pure polymers. These characteristics, combined with the very high antibacterial activity previously reported, suggest these materials are suitable for use as catheter materials.

Acknowledgements M.W., J.P. and I.P.P. thank the BBSRC for supporting this work through grant BB/E012310/1; I.P.P. thanks the Royal Society/Wolfson trust for a merit award.

References

1. Rabinowicz E. Friction and wear of materials. New York: Wiley; 1965.
2. Greenwood JA. Contact of rough surfaces. In: Singer IL, Pollock HM, editors. Fundamentals of friction: macroscopic and microscopic processes. Dordrecht: Kluwer; 1992. p. 37–56.
3. Bowden F, Tabor D. The friction and lubrication of solids. Oxford: Clarendon Press; 1986.
4. Bhushan B. Introduction to tribology. New York: Wiley; 2002.
5. Amontons G. De la resistance caus'ee dans les machines. Me′moires de l'Acade′mie Royale. 1699;A:257–82.
6. Gao J, Luedtke WD, Gourdon D, Ruth M, Israelachvili JN, Landman U. Frictional forces and Amonton's law: from the molecular to the macroscopic scale. J Phys Chem B. 2004;108:3410–25.
7. Persson BNJ, Tosatti E. Physics of sliding friction. Dordrecht: Kluwer Academic; 1996.
8. Stickler DJ, Lear JC, Morris NS, Macleod SM, Downer A, Cadd DH, et al. Observations on the adherence of Proteus mirabilis onto polymer surfaces. J Appl Microbiol. 2006;100:1028–33.
9. Ferrieres L, Hancock V, Klemm P. Specific selection for virulent urinary tract infectious *Escherichia coli* strains during catheter-associated biofilm formation. FEMS Immunol Med Microbiol. 2007;51:212–9.
10. Norwood DE, Gilmour A. The growth and resistance to sodium hypochlorite of *Listeria monocytogenes* in a steady-state multispecies biofilm. J Appl Microbiol. 2000;88:512–20.
11. Juan-Torres A, Harbarth S. Prevention of primary bacteraemia. Int J Antimicrob Agents. 2007;30S:S80–7.
12. Haa US, Chob YH. Catheter-associated urinary tract infections: new aspects of novel urinary catheters. Int J Antimicrob Agents. 2006;28:485–90.
13. Hetrick EM, Schoenfisch MH. Reducing implant-related infections: active release strategies. Chem Soc Rev. 2006;35:780–9.
14. Perni S, Piccirillo C, Pratten JR, Prokopovich P, Chrzanowski W, Parkin IP, et al. The antimicrobial properties of light-activated polymers containing methylene blue and gold nanoparticles. Biomaterials. 2009;30(1):89–93.
15. Perni S, Prokopovich P, Piccirillo C, Pratten JR, Parkin IP, Wilson M. Toluidine blue-containing polymers exhibit bactericidal activity when irradiated with red light. J Mater Chem. 2009;19:2715–23.
16. Jones DS, Garvin CP, Gorman SP. Relationship between biomedical catheter surface properties and lubricity as determined using textural analysis and multiple regression analysis. Biomaterials. 2004;25:1421–8.
17. Jones DS, Garvin CP, Gorman SP. Design of a simulated urethra model for the quantitative assessment of urinary catheter lubricity. J Mater Sci Mater Med. 2001;12:15–21.
18. Ho SP, Nakabayashi N, Iwasaki Y, Boland T, LaBerge M. Frictional properties of poly(MPC-co-BMA) phospholipid polymer for catheter applications. Biomaterials. 2003;24:5121–9.

19. D'Angelo E, Loring SH, Gioia ME, Pecchiari M, Moscheni C. Friction and lubrication of pleural tissues. Respir Physiol Neurobiol. 2004;142(1):55–68.
20. Takashima K, Shimomura R, Kitou T, Terada H, Yoshinaka K, Ikeuchi K. Contact and friction between catheter and blood vessel. Tribol Int. 2007;40:319–28.
21. Kazmierska K, Szwast M, Ciach T. Determination of urethral catheter surface lubricity. J Mater Sci Mater Med. 2008;19:2301–6.
22. Karaszkiewicz A. Contact width and contact pressure of o-seals. Przegl Mech. 1979;7:14–6, 25–6 (in Polish).
23. Triolo PM, Andrade JD. Surface modification and characterization of some commonly used catheter materials. II. Friction characterization. J Biomed Mater Res. 1983;17:149–65.
24. Homola AW, Israelachvili JN, McGuiggan PM, Lee ML. Fundamental experimental studies in tribology: the transition from interfacial friction of undamaged molecularly smooth surfaces to normal friction with wear. Wear. 1990;136:65–83.
25. Schwarz UD, Zworner O, Koster P, Wiesendanger R. Quantitative analysis of the frictional properties of solid materials at low loads. Carbon compounds. Phys Rev B. 1997;56:6987–96.
26. Blau PJ. Scale effect in steady-state friction. Tribol Trans. 1991;34:335–42.
27. Hurtado J, Kim K. Scale effect in friction of single-asperity contacts. 1. From concurrent slip to single-dislocation-assisted slip. II. Multiple-dislocations-cooperated slip. Proc R Soc Lond A. 1999;455:3363–400.
28. Johnson KE. Histology and cell biology. Baltimore, MD: Williams and Wilkins; 1991.
29. Stensballe J, Looms D, Nielsen PN, Tvede M. Hydrophilic-coated catheters for intermittent catheterisation reduce urethral micro-trauma: a prospective, randomised, participant-blinded, crossover study of three different types of catheters. Eur Urol. 2005;48:978–83.
30. Koga S, Ikeda S, Futagawa K, Sonoda K, Yoshitake T, Miyahara Y, et al. The use of a hydrophilic-coated catheter during transradial cardiac catheterization is associated with a low incidence of radial artery spasm. Int J Cardiol. 2004;96(2):255–8.